biomolecules

MDPI

*Article*

# DERA-Catalyzed Chemoenzymatic Access to Nucleobase-Substituted Candidate Statin Precursors

**Romina Fernández Varela [1,†], Eman Abdelraheem [2,†], Lautaro Giaimo [1], Luciano Cortés [1], Leticia Lafuente [1], Ana Laura Valino [1], Peter-Leon Hagedoorn [2], Ulf Hanefeld [2], Adolfo Iribarren [1] and Elizabeth Lewkowicz [1,*]**

[1] Laboratorio de Biotransformaciones y Química de Ácidos Nucleicos, Universidad Nacional de Quilmes, Consejo Nacional de Investigaciones Científicas y Técnicas (CONICET), Roque S. Peña 352, Bernal B1876BXD, Argentina; rnfernandezvarela@gmail.com (R.F.V.); lautarog.lg@gmail.com (L.G.); luciano.i.cortes@gmail.com (L.C.); leti.lafuente@gmail.com (L.L.); avalino@unq.edu.ar (A.L.V.); airibarren@unq.edu.ar (A.I.)

[2] Biocatalysis Group, Department of Biotechnology, Delft University of Technology, Van der Maasweg 9, 2629 HZ Delft, The Netherlands; eabdelraheem93@gmail.com (E.A.); p.l.hagedoorn@tudelft.nl (P.-L.H.); u.hanefeld@tudelft.nl (U.H.)

* Correspondence: elewko@unq.edu.ar

† These authors contributed equally to this work.

## Abstract

Aldolases are powerful biocatalysts for the stereoselective formation of carbon–carbon bonds and are widely used in the synthesis of chiral intermediates for pharmaceutical applications. Among them, 2-deoxyribose-5-phosphate aldolase (DERA) has been extensively exploited for the preparation of the conserved side chain of statins. In this work, we report a novel chemoenzymatic approach for the synthesis of nucleobase-substituted lactol products as potential precursors of new statin analogues. A C49M variant of DERA from *Pectobacterium atrosepticum* (*Pa*DERA C49M) was employed to catalyze sequential aldol additions using aldehyde-functionalized nucleobases as non-natural electrophilic substrates. The formation of nucleobase-containing lactols was confirmed, demonstrating for the first time the acceptance of nucleobase-derived aldehydes in DERA-catalyzed aldol reactions. This strategy provides access to structurally novel statin side-chain precursors and expands the synthetic potential of DERA toward the generation of new classes of bioactive compounds.

**Keywords:** 2-deoxyribose-5-phosphate aldolase (DERA); *Pectobacterium atrosepticum*; aldol addition; statins; nucleobases



Academic Editor: Bartłomiej Zieniuk

Received: 22 January 2026
Revised: 12 February 2026
Accepted: 13 February 2026
Published: 19 February 2026



## 1. Introduction

Cardiovascular disease remains the leading cause of mortality worldwide, with over 20 million deaths annually [1,2]. Among the established risk factors associated with its global health impact—including low physical activity, obesity, diabetes, smoking and high blood pressure—elevated low-density lipoprotein (LDL) cholesterol represents a major determinant, implicated in approximately 3.8 million deaths [3].

Statins are usually prescribed to reduce the levels of LDL cholesterol through inhibition of the rate-limiting enzyme 3-hydroxy-3-methylglutaryl-coenzyme A (HMG-CoA) reductase involved in the conversion of HMG-CoA to mevalonate, which is an early step in the synthesis of cholesterol [4]. Since the discovery of the first cholesterol biosynthesis inhibitor, Mevastatin, in the 1970s, statin families have expanded rapidly through the development of natural, semisynthetic, and fully synthetic statins (Figure 1) [5]. Although

statins are generally well-tolerated and safe, adverse reactions become more significant as the number of users increases. These often include muscle weakness, hepatic damage, renal insufficiency, and the potential to induce diabetes. For this reason, there is growing interest in finding alternatives that minimize these effects [6,7].

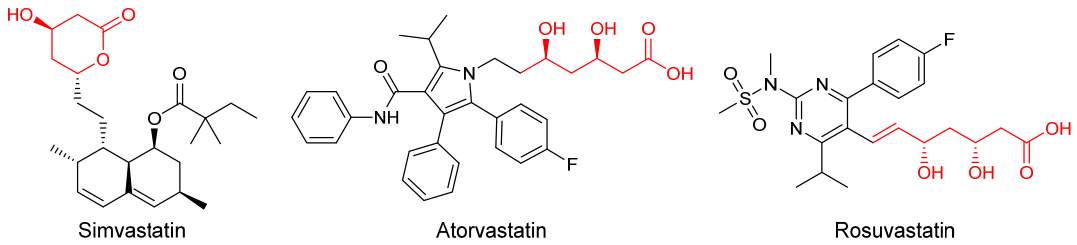


**Figure 1.** Some U.S. Food & Drug Administration (FDA)-approved statins.

The aldol reaction is an important tool in biological systems and in organic chemistry to produce carbon skeletons, with aldolases being the most suitable enzymes to catalyze this reaction in an asymmetric way [8,9]. In particular, 2-deoxyribose-5-phosphate aldolase (DERA) catalyzes the stereoselective aldol addition between two aldehydes via an enamine intermediate, the typical mechanism of Class I aldolases [10]. This enzyme is strictly dependent on acetaldehyde as a nucleophile but can accept a wide range of aldehydes as electrophiles, producing 2,4,6-trideoxyhexoses (Scheme 1). This sequential aldol addition is thermodynamically controlled and stops when a stable intramolecular hemiacetal is formed [11]. The two chiral centers generated, controlled by the enzyme [12], have the appropriate stereochemistry for the cyclic hemiacetal (lactol) to be used as intermediates in the production of Atorvastatin and other related cholesterol-lowering drugs [13–15]. However, the application of DERA in large-scale production of these pharmaceutical compounds is limited by some drawbacks, such as low catalytic activity and low tolerance to aldehydes [16]. To overcome this disadvantage, different technologies such as directed evolution, protein engineering, computational design, and immobilization have been applied to improve DERA's properties [17]. In particular, a number of recombinant DERA variants with increased productivity, from mesophilic [18], psychrophilic [19], and thermophilic organisms [20], have been reported.

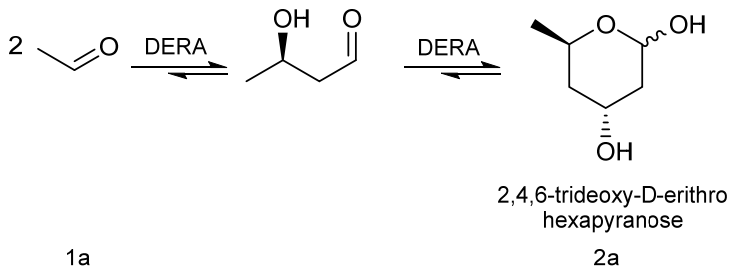


**Scheme 1.** Sequential aldol addition by DERA.

The most efficient modification to provide acetaldehyde resistance involves the mutation of a cysteine, non-essential for catalysis (C47 in DERA from *E. coli*), by a non-nucleophilic amino acid such as methionine, which avoids the formation of a bridge via a Michael addition of crotonaldehyde, resulting from the condensation of two acetaldehyde molecules with the lysine K167 in the active site [16]. In this regard, *Ec*DERA C47M showed no loss of activity after incubation in 300 mM of acetaldehyde for 16 h, in contrast to wild-type *Ec*DERA, which was completely inactivated after 3 h [21]. Similar behavior was observed in DERAs from *Lactobacillus brevis* [22], *Rhodococcus erythropolis* strain DSM 311 [23], *Thermotoga maritima* [24], archaeon *Pyrobaculum aerophilum* [25] and *Staphylococcus*

*aureus* [26], among others, after cloning, modification and recombinant expression in *E. coli*. Previous work in our lab involved DERA from *Pectobacterium atrosepticum* ATCC 33,260 (*Pa*DERA) [27], which was genetically modified, cloned and expressed in *E. coli*. In comparison to the wild-type enzyme, *Pa*DERA C49M (which corresponds to C47 in *Ec*DERA) retained 90% of its activity after incubation for 90 min in 300 mM of acetaldehyde [28].

Different 6-substituted 2,4,6-trideoxy-D-erythro hexapyranoses (6-*R*-TDHP) were reported over time as precursors of the side chain of statins. (3*R*,5*S*)-6-chloro-2,4,6-trideoxyhexapyranoside (ClTDHP) was the first biocatalytically synthesized intermediate using diverse DERA variants. This approach represented a great improvement, in chemical and stereochemical purity and cheap achiral starting materials, over its chemical synthesis [29–33]. This biotransformation has been successfully used to prepare the statin side-chain of Rosuvastatin on a manufacturing scale [34]. Besides chlorine, acetoxy [35], azido [36] and *N*-protected amino [37] groups were reported as TDHP 6-substituents in order to improve productivity. Švarc et al. [34] developed an alternative strategy in which aminophenylacetamide-protected propanal is used as the starting aldehyde of the aminolactol precursor of Atorvastatin. Lactols can then be oxidized to the corresponding lactones, after which further chemical steps attach them to the heterocycle moiety to obtain the different statins [5,38,39].

The conserved 3,5-dihydroxyheptanoic acid moiety present in all statins is responsible for HMG-CoA reductase inhibition through competitive and reversible binding due to its structural similarity to its natural substrate, HMG-CoA. In addition, interactions between the enzyme and the remaining portions of the molecule contribute to binding affinity [40]. While natural statins contain a hexahydronaphthalene core, synthetic statins incorporate diverse heterocyclic structures, such as pyrrole in Atorvastatin, pyrimidine in Rosuvastatin, or quinoline in Pitavastatin [41]. Accordingly, drug development efforts aimed at improving efficacy and tolerability have primarily targeted the heterocyclic scaffold [42].

Unlike statins, eritadenine, an acyclic adenosine analog with hypocholesterolemic activity, does not affect cholesterol production but accelerates cholesterol metabolism in the liver, modifying phospholipid metabolism and promoting the removal of cholesterol from the blood through mechanisms that increase LDL cholesterol uptake [43,44]. This led us to consider the possibility of preparing statins containing a nucleoside base, such as the heterocycle. Therefore, the objective of this work was to generate the side chain precursors for new statin analogues from aldehyde derivatives of nitrogen bases, using *Pa*DERA C49M, recently cloned and overexpressed by us, and whose synthetic activity towards the formation of TDHP has already been reported [45].

## 2. Materials and Methods

### *2.1. Chemicals and Microorganisms*

Reagents and substrates were purchased from Sigma-Aldrich (St Louis, MO, USA). TLC analysis was performed using silica gel 60 F254 aluminum plates from Merck (Darmstadt, Germany). The culture media components were obtained from Anedra (Buenos Aires, Argentina), Britania (Buenos Aires, Argentina) and Sigma-Aldrich. Solvents were from Sintorgan (Buenos Aires, Argentina) and Biopack (Zárate, Argentina). *Escherichia coli* DH5α (Invitrogen, Thermo Fisher Scientific, Waltham, MA, USA) and *E. coli* BL21 (DE3) (ATCC 47092, acid phosphatase-deficient) strains were used in cloning and expression experiments.

### *2.2. Culture Conditions*

Plasmids encoding *P. atrosepticum* DERA, including the mutation C49M (*Pa*DERA C49M), as described in ref. [28], were transformed into chemically competent *E. coli* BL21

(DE3) for expression. Each recombinant *E. coli* strain was grown in LB medium supplemented with kanamycin 30 μg/μL at 37 °C and 200 rpm overnight. The pre-cultures (25 mL) were then used to inoculate a fresh LB medium containing kanamycin 30 μg/μL (250 mL) and grown at 37 °C, 200 rpm until $OD_{600}$ reached 0.6–0.8, at which point the protein expression was induced with isopropyl-*β*-thiogalactoside (IPTG) at a final concentration of 0.1 mM. The cultures continued growing at 28 °C and 180 rpm overnight. Subsequently, the cells were harvested by centrifugation (5000 rpm, 10 min, 4 °C), washed with 0.1 M potassium phosphate buffer pH 7.0, recentrifuged and used as whole cell biocatalysts ($2.5 \times 10^9$ cells/mg wet weight) or to continue towards protein purification.

### 2.3. Enzyme Purification

*E. coli* (*Pa*DERA C49M) cells were resuspended in 0.1 M potassium phosphate buffer, pH 7, to achieve a final concentration of 30% *w*/*v*. The suspension was sonicated at 50% amplitude for four cycles at 4 °C using the Vibra Cell disruptor (VCX130, Sonics, Newtown, CT, USA) or incubated with lysozyme (1 mg/g wet weight of cells) for 24 h at 4 °C and 200 rpm. The suspension was centrifuged at 4 °C and 9000 rpm for 15 min, and the supernatant was conserved as cell-free extract (CFE).

For the enzyme purification by batch-mode affinity chromatography, 20 mL of *Ni*-Sepharose TM 6 Fast Flow resin (obtained from GE Life Science, Boston, MA, USA) and 20 mL of CFE were incubated for 1 h at 4 °C. After that, the solid phase (resin with bound enzyme) was separated from the supernatant by centrifugation, and the unbound CFE was discarded. The resin was then subjected to sequential washing–centrifugation steps with imidazole solutions at increasing concentrations (5 mM–500 mM). Relevant fractions of the eluted proteins were combined, desalted and concentrated to a final volume of 1 mL by centrifuging at 5700 rpm at 4 °C in a Vivaspin 20 Centrifugal Concentrator (Sartorius, Göttingen, Alemania).

### 2.4. Activity Assay and Determination of Protein Concentration

The activity of *Pa*DERA C49M was determined by the coupled assay described previously [46], measuring the oxidation of NADH. The assay mixture contained 0.1 M potassium phosphate buffer, pH 7.0, 0.2 mM NADH, 0.4 mM 2-deoxyribose-5-phosphate (DR5P), 4 μL of the mixture *α*-glycerophosphate dehydrogenase/triosephosphate isomerase (*α*-GDH-TPI) and 5 μL of purified protein. The reaction was initiated by the addition of purified protein and the subsequent decrease of NADH concentration was monitored at 340 nm. A total of 1 U of protein activity was defined as the amount of enzyme required for cleavage of 1 μmol of DR5P per minute at 28 °C. The protein concentration was determined by the Bradford assay [47]. *Pa*DERA C49M protein concentration: 0.98 mg/mL and *Pa*DERA C49M activity: 28.9 U/mg.

### 2.5. Substrate Synthesis

*N*-1-(2,2-dimethoxyethyl) thymine (**4i**), *N*-1-(2,2-dimethoxyethyl) cytosine (**4ii**), and *N*-9-(2,2-dimethoxyethyl) adenine (**4iii**) were prepared according to our previous report [48]. Mixtures of thymine (**3i**), cytosine (**3ii**) or adenine (**3iii**) (1 equiv.) and $K_2CO_3$ (2 equiv.) in DMF (10 mL) were stirred at 90 °C in the presence of 2-bromo-1,1-dimethoxy ethane (2 equiv.). After 24 h, the reactions were filtered and the solvent was removed under reduced pressure. The crude mixtures were purified by column chromatography on silica gel (230 mesh), using approximately 40% *w*/*w* of crude material relative to the stationary phase. Elution was performed using dichloromethane/methanol as the mobile phase, gradually increasing the polarity. Column progress was monitored by TLC, using dichloromethane/methanol (9:1) as the eluent. Aldehydes (*N*-1-(2-oxoethyl) thymine (**5i**), *N*-1-(2-oxoethyl) cytosine (**5ii**) or *N*-9-(2-oxoethyl) adenine (**5iii**) were obtained after hy-

drolysis of the corresponding acetals (**4i-iii**) in HCl (1 N) at 90 °C for 1 h and neutralization with NaOH (2 N). NMR and ESI-MS spectral characteristics are in accordance with the literature [49].

### *2.6. Whole Cell Biotransformations*

#### 2.6.1. Synthesis of 2,4,6-Trideoxy-D-Erythro-Hexapyranose (TDHP, **2a**)

The reactions were performed in a 4 mL final volume, 100 mM potassium phosphate buffer, pH 7, carrying 1 M of acetaldehyde and $2.5 \times 10^9$ *E. coli* (*Pa*DERA C49M) cells/mg wet weight as biocatalyst. The reaction mixture was shaken at 28 °C and 200 rpm for 24 h and then centrifuged for 10 min at 5000 rpm. The supernatant was extracted with 2 volumes of ethyl acetate and purified by silica gel column chromatography using ethyl acetate as eluent. The NMR data are in accordance with the literature [45].

#### 2.6.2. Synthesis of 6-Substituted-2,4,6-Trideoxy-D-Erythro-Hexapyranoses (**2b-e**)

The reactions were performed in a 4 mL final volume, 100 mM potassium phosphate buffer, pH 7, carrying 100 mM of chloroacetaldehyde (**1b**), propanaldehyde (**1c**), phenylacetaldehyde (**1d**) or benzaldehyde (**1e**) as acceptors, acetaldehyde 200 mM as donor, and $2.5 \times 10^9$ *E. coli* (*Pa*DERA C49M) cells/mg wet weight as biocatalyst. The reaction mixtures were shaken at 28 °C and 200 rpm for 24 h and then centrifuged for 10 min at 5000 rpm. The supernatants were extracted with 2 volumes of ethyl acetate, purified by silica gel column chromatography using ethyl acetate as eluent and analyzed by GC.

### *2.7. Free-Enzyme Biotransformation*

#### Synthesis of 6-Substituted Lactols (**6i-iii**)

The reactions were carried out in a final volume of 1 mL of 0.1 M potassium phosphate buffer (pH 7), containing 100 mM (**5i**, **5ii**, **5iii**) as the acceptors, 100 mM acetaldehyde as the donor, and 1 mg/mL *Pa*DERA C49M. The reaction mixtures were shaken at 28 °C and 200 rpm for 24 h. Subsequently, the reactions were quenched with acetonitrile and centrifuged at 11,000 rpm for 3 min. The resulting supernatants were extracted three times with one volume of ethyl acetate. Compounds **6i-iii** were analyzed by HPLC-UV/MS. Compound **6i** was isolated from an 8 mL reaction mixture through extensive extraction with ethyl acetate and subsequently purified by silica gel (230 mesh) column chromatography employing dichloromethane/methanol (9:1) as the mobile phase.

### *2.8. Analytical Methods*

#### Instrumental

The progress of the reactions and the conversion of substrates **5i–iii** were monitored by analytical HPLC–UV using a Gilson chromatograph (321 pump, 156 UV/VIS detector, and 234 series autoinjector; Middleton, WI, USA). Separations were performed on a SiliaChrom SB RP18 column (150 × 4.6 mm, 5 µm; Quebec City, QC, Canada). Water (A) and acetonitrile (B) were used as mobile phases at a flow rate of 0.9 mL·min$^{-1}$. The elution program was as follows: 4 min at 99% A and 1% B; a linear gradient over 3 min to 88% A and 12% B; 5 min at 88% A and 12% B; followed by a linear gradient over 3 min back to 99% A and 1% B.

Gas chromatography (GC) analyses of the biotransformations of compounds **1a–e** were performed using a Thermo Scientific Trace 1300 gas chromatograph (Thermo Fisher Scientific) equipped with a TR-5 capillary column (30 m × 0.25 mm × 0.25 µm), using helium as carrier gas (1 mL/min). The injector temperature was set at 200 °C, and the oven temperature program was 50 °C for 5 min, ramped to 250 °C at 10 °C/min, and held at the final temperature for 5 min.

Structural characterization of all isolated compounds was carried out by $^{1}H$ and $^{13}C$ NMR spectroscopy on Bruker Avance II 500 and Avance III 600 spectrometers (Madison, WI, USA), operating at 500/125 MHz and 600 MHz, respectively, using $CDCl_3$ as solvent.

High-resolution mass spectra of 6-substituted lactols (**6i-iii**) were recorded using an ACQUITY UPLC system (Waters, Milford, MA, USA) coupled to an Orbitrap mass spectrometer (Q-Exactive Focus, Thermo Fisher Scientific,). Chromatographic separation was achieved on a reverse-phase ACQUITY UPLC BEH C18 column (1.0 × 100 mm, 1.7 µm; Waters, UK) at room temperature. The mobile phases consisted of water containing 0.1% formic acid (A) and acetonitrile containing 0.1% formic acid (B), using a flow rate of 50 µL/min. The gradient started at 5% B for 15 min, increased to 75% B over 22 min, and then returned to initial conditions for re-equilibration. The mass spectrometer was operated in positive ESI mode, alternating between full scan (50–750 $m/z$, resolution 70 K) and PRM mode. Data were analyzed using XCalibur 4.1 software.

Enzymatic activity and other spectrophotometric assays were performed using a Shimadzu UV-160A UV–visible spectrophotometer (Shimadzu, Kyoto, Japan).

### *2.9. $^{1}H$ and $^{13}C$ NMR Product Data*

All chromatographic and spectral data are available in the Supplementary Materials (SM) file.

2,4,6-trideoxy-D-erythro-hexapyranose (**2a**) [45]

$^{1}H$ NMR (600 MHz, $CDCl_3$) δ (ppm) 5.34 (t, $J$ = 4.7 Hz, 1H, α, H-1), 5.22–5.12 (m, 1H, β, H-1), 4.44 (dtd, $J$ = 12.4, 6.3, 2.4 Hz, 1H, α/β, H-5), 4.35 (q, $J$ = 3.1 Hz, 1H, β, H-5), 4.24 (dt, $J$ = 6.4, 3.1 Hz, 1H, α, H-3), 4.10 (qd, $J$ = 5.7, 5.2, 2.0 Hz, 1H, β, H-3), 4.07 (d, $J$ = 6.5 Hz, 1H, α, H-4a), 3.17 (d, $J$ = 6.1 Hz, 1H, β, H-4a), 3.01 (d, $J$ = 6.5 Hz, 1H, α, H-4b), 2.05–1.95 (m, 1H, α/β, H-4b), 1.88–1.76 (m, 2H, α/β, H's-2a), 1.56 (ddd, $J$ = 14.2, 11.7, 2.7 Hz, 1H, α, H-2b), 1.48 (ddd, $J$ = 14.2, 11.5, 2.9 Hz, 1H, β, H-2b), 1.26 (d, $J$ = 6.3 Hz, 3H, β, H's-6), 1.24 (d, $J$ = 6.3 Hz, 3H, α, H's-6).

$^{13}C$ NMR (126 MHz, $CDCl_3$) δ (ppm): 94.3 (CHOH, C-1), 93.0 (CHOH, C-1′), 68.3 (CH, C-5), 66.8 (CH, C-5′), 65.1 (CHOH, C-3), 64.1 (CHOH, C-3′), 42.8 ($CH_2$, C-2), 42.3 ($CH_2$, C-2′), 39.9 ($CH_2$, C-4), 39.1 ($CH_2$, C-4′), 21.4 ($CH_3$, C-6), 21.2 ($CH_3$, C-6′).

6-chloro-2,4,6-trideoxy-D-erythro-hexapyranose (**2b**) [15]

$^{1}H$ RMN (500 MHz, $CDCl_3$): δ (ppm) 5.51 (d, $J$ = 3.5 Hz, 1H, β, H-1), 5.41 (d, $J$ = 3.6 Hz, 1H, α, H-1), 4.53 (dd, $J$ = 9.0, 4.2 Hz, 1H, H-5), 4.32 (m, 1H, H-5'), 4.28–4.18 (m, 1H, H-3'), 3.91 (dq, $J$ = 11.7, 6.2 Hz, 1H, H-3), 3.63–3.55 (m, 4H, H's-6), 2.22–1.74 (H-4, H-4', H-2b, H-2'b), 1.55 (td, $J$ = 12.0, 3.6 Hz, 1H, H-2a), 1.47–1.28 (m, 1H, H-2'a).

$^{13}C$ NMR (126 MHz, $CDCl_3$) δ (ppm): 93.1 (CHOH, C-1), 92.9 (CHOH, C-1′), 68.0 (CH, C-5), 64.6 (CH, C5′), 63.1 (CHOH, C-3), 63.1 (CHOH, C-3′), 47.7 ($CH_2$, C-6), 47.2 ($CH_2$, C-6′), 39.0 ($CH_2$, C-2), 38.3 ($CH_2$, C-2′), 35.4 ($CH_2$, C-4), 34.8 ($CH_2$, C-4′).

6-thyminyl-2,4,6-trideoxy-D-erythro-hexapyranose (**6i**)

$^{1}H$ NMR (500 MHz, DMSO-$d_6$): δ (ppm) 11.25 (d, $J$ = 12.5 Hz, 1H, NH), 7.44 (s, 1H, H-7), 4.85 (d, $J$ = 9.1 Hz, 1H, H-1), 4.08 (s, 1H, H-3), 4.03 (d, $J$ = 8.6 Hz, 1H, H-5), 3.74 (d, $J$ = 3.5 Hz, 1H, H-6a), 3.58 (d, $J$ = 8.4 Hz, 1H, H-6b), 1.75 (s, 3H, H-9), 1.68 (d, $J$ = 14.0 Hz, 1H, H-2b), 1.47 (d, $J$ = 12.7 Hz, 1H, H-4a), 1.34 (t, $J$ = 11.6 Hz, 1H, H-2a), 1.26 (d, $J$ = 11.6 Hz, 1H, H-4b).

$^{13}C$ NMR (126 MHz, DMSO-$d_6$): δ (ppm): 164.8 (CO, C-11), 151.4 (CO, C-10), 143.0 (CH, C-7), 108.1 (CH, C-8), 92.1 (CHOH, C-1), 68.3 (CH, C-5), 63.7 (CHOH, C-3), 52.15 ($CH_2$, C-6), 40.2 ($CH_2$, C-2), 35.4 ($CH_2$, C-4), 12.4 ($CH_3$, C-9).

$m/z$ found: 257.1124, estimated $[C_{11}H_{17}N_2O_5]^+$: 257.2634.

## 3. Results and Discussion

The chemical synthesis of statins presents several drawbacks, including modest overall yields, the use of large amounts of hazardous reagents, and the generation of considerable chemical waste [50]. Furthermore, the stereoselective construction of the chiral centers in the side chain, the main pharmacophoric motif, is particularly challenging. In contrast, the use of biocatalysts offers advantages such as high regio and stereo selectivity, use of non-polluting raw materials and solvents, and mild reaction conditions, which help to reduce costs and improve sustainability [51]. Among the different biocatalysts used to synthesize the conserved chiral side chain of statins [52], DERA is one of the most studied because it has the ability to simultaneously generate both stereocenters from simple aldehydes [5].

### *3.1. Expression and Purification of PaDERA C-His AA C49M*

*Pectobacterium atrosepticum* ATCC 33,260 DERA (*Pa*DERA) [27] was cloned and expressed as previously reported [28]. The variant *Pa*DERA C49M, including a C-terminal 6×His tag, a 5-amino-acid spacer, and the C49M mutation, was selected due to its high activity in the presence of acetaldehyde [28,45]. To enable the use of free *Pa*DERA C49M as a biocatalyst, the enzyme was purified from a crude cell-free extract (CFE) obtained by enzymatic or mechanical lysis. Both methods gave comparable enzyme recovery and catalytic activity; however, only enzymatic lysis preserved the expected stereoselectivity. Mechanical disruption led to a marked loss of stereocontrol, likely due to structural perturbations, as reported for other aldolases [53].

Purification was performed by batch-mode affinity chromatography, since column-based purification caused complete loss of enzymatic activity. This behavior is likely linked to the high flexibility of the C-terminal region [54], which may be incompatible with prolonged Ni–NTA binding conditions [55]. Batch-mode purification reduces resin contact time, preserving enzymatic activity and also providing sufficient material for subsequent reactions. After the purification, the enzyme displayed an initial specific activity of 28.9 U/mg; however, activity declined to 17.19 U/mg after 24 h at 4 °C and was completely lost after 48 h. Limited stability of isolated DERAs has been widely reported, and although approaches such as protein engineering and enzyme immobilization have been investigated, improving their stability continues to be challenging [32,56].

### *3.2. PaDERA C-His AA C49M and Chiral Lactols*

The use of whole-cell biocatalysts represents an attractive alternative for industrial processes, not only because of their low production cost, but also because they help mitigate stability issues and circumvent the need for laborious enzyme purification. *E. coli* (*Pa*DERA C49M) was employed as a whole-cell biocatalyst to prepare 2,4,6-trideoxy-D-erythro-hexapyranose (TDHP, **2a**) in 99% yield by tandem aldol addition of acetaldehyde even at concentration of 500 mM [45].

To validate the potential of the new mutant as a versatile whole-cell biocatalyst, we performed a DERA-catalyzed aldol addition using acetaldehyde as donor and different acceptor aldehydes, as shown in Table 1. Chloroacetaldehyde (**1b**) was the first substrate studied and used in DERA-catalyzed reactions. Moreover, it is the most widely industrially employed due to the versatility of chlorine to participate in subsequent reactions to introduce the heterocycle moiety to statins preparation [52,57]. Additionally, propanaldehyde (**1c**), phenylacetaldehyde (**1d**) and benzaldehyde (**1e**) allowed us to explore the acceptance of non-phosphorylated electrophilic substrates by DERA, non-polar, bulky and aromatic respectively. None of the substrates was as good as **1a** for *Pa*DERA C49M. As usual, aromatic aldehydes were not substrates for the enzyme [54]. Recently, Rizzo et al. [53], using metagenomic technology for enzyme discovery, reported for the first time a DERA capable

of accepting furfural and benzaldehyde with higher activity and stereoselectivity than those achieved with other well-known DERAs with non-natural substrates.

**Table 1.** 6-substituted lactols synthesized by *E. coli* (*Pa*DERA C49M) [a].

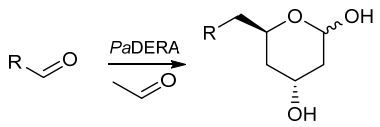


**1a-e** **2a-e**

| | | | | | |
|---|---|---|---|---|---|
| Acceptor aldehyde |  **1a** | 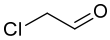 **1b** | 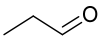 **1c** | 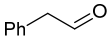 **1d** |  **1e** |
| Lactol product | 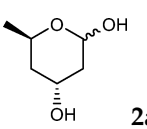 **2a** | 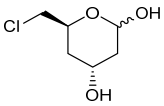 **2b** | 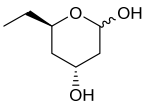 **2c** | 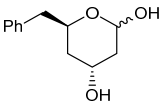 **2d** | 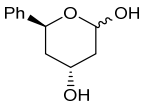 **2e** |
| Yield (%) | 99 | 33 | 22 | 28 | <5 |

[a] Reactions performed with 100 mM potassium phosphate buffer, pH 7, carrying 100 mM of **1a-e**, 200 mM acetaldehyde and 2.5 × $10^9$ *E. coli* (*Pa*DERA C49M) cells/mg wet weight as biocatalyst. The reaction mixtures were shaken at 28 °C and 200 rpm for 24 h.

All biotransformations were carried out using experimental conditions previously optimized for the synthesis of **2a** [45]. After biotransformations, lactols **2b-e** were extracted with ethyl acetate and further purified by silica column chromatography. Due to their instability and the presence of byproducts, the purification was quite problematic. Indeed, given the difficulty of purifying these compounds, most reports that employ them as intermediates utilize the crude product [16]. All compounds were quantified by GC, observing the presence of TDHP as a secondary product, a pattern that was maintained in all aldol biotransformations. Only **2b** was isolated and analyzed by $^1$H and $^{13}$C NMR, which were consistent with previous reports [33,45]. The presence of both anomers was corroborated by the duplication of signals in both spectra and, in particular, by the signals corresponding to the hydrogens bonded to the anomeric carbons of the two anomers at 5.41 ppm and 5.51 ppm of the $^1$H NMR spectrum with a 7:3 (α/β) ratio (Figures S6 and S7).

### *3.3. Novel Statin Precursors*

As previously mentioned, traditional statin synthesis involves the construction of the functionalized chiral side-chain with a reactive group (e.g., chloro, cyano, or acetoxy), which then serves as a building block for introducing the corresponding heterocycle [54]. For over two decades, our laboratory has focused on the synthesis of nucleoside analogues using biocatalytic approaches. In recent years we have explored the use of different aldolases as biocatalysts for the synthesis of acyclic nucleoside analogues employing aldehyde-functionalized nucleobases as key precursors [48,58,59]. In line with these efforts, we implemented a chemoenzymatic strategy aimed at generating novel nucleobase-containing statin candidates. This approach comprises the synthesis of suitably functionalized aldehyde nucleobases, their conversion into the corresponding substituted lactols through *Pa*DERA C49M catalysis, and a final oxidation step affording the target lactone (Scheme 2).

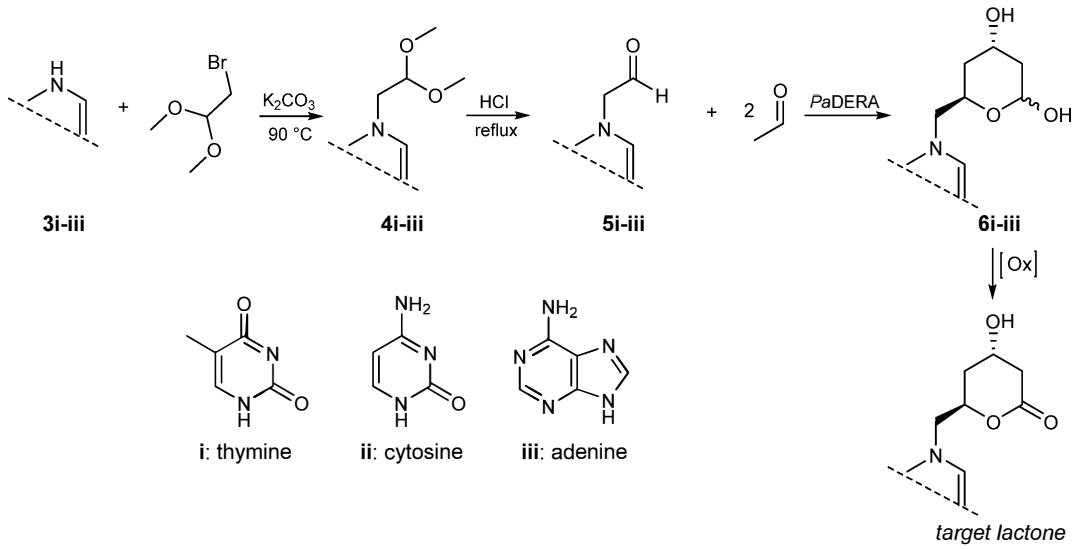


**Scheme 2.** Chemoenzymatic approach to nucleobase-containing lactol precursors (**6i-iii**) of potential statins.

Compounds **5i–iii** were obtained by *N*-alkylation of the corresponding bases **3i–iii**, followed by acid hydrolysis of the acetal intermediates **4i–iii**, as previously reported [49]. The resulting aldehydes were then added to a phosphate-buffered solution containing *E. coli* (*Pa*DERA C49M) whole cells and acetaldehyde, which serves as the specific donor. Upon substrate consumption, analysis of the crude reaction mixture and the extracted supernatant revealed several low-abundance, hard-to-purify byproducts, most likely originating from biocatalyst-mediated substrate decomposition.

In light of these results, the crude cell-free extract (CFE) obtained from disrupted *E. coli* (*Pa*DERA C49M) whole cells was tested as a biocatalyst. This strategy did not lead to improved outcomes, as the small amount of the product formed exhibited degradation after 3 h of reaction. However, the appearance of the product allowed us to determine that aldehydes **5i-iii** were substrates of DERA and that, probably due to their structures being similar to natural nucleosides, they could also be substrates for other enzymes present in the CFE. Therefore, the use of free purified *Pa*DERA C49M as a biocatalyst for this biotransformation was necessary.

The enzyme was purified as described above and used immediately to minimize storage instability. The amount of enzyme used (1 mg/mL) was equivalent to the biocatalyst loading employed in the other formats. In order to reduce the formation of TDHP as a by-product, the **1a:5i-iii** ratio was adjusted to 1:1. However, the strong preference of **1a** as both donor and acceptor substrate made this unavoidable, and TDHP formation was still observed. Additionally, the presence of TDHP further increased the intrinsic difficulty of product purification, as is commonly observed for nucleobase derivatives.

The biotransformation was performed in a buffered solution containing substrates and the enzyme. Reaction progress was monitored by TLC and HPLC, and upon completion, the formation of products **6i-iii** was confirmed by HPLC–MS (Figures S20–S22).

As discussed above, the purification of lactol products from reaction mixtures is challenging due to the instability of the hemiacetal moiety, the coexistence of anomeric forms, and the poor solubility of nucleoside bases in organic solvents. In addition, when DERA is employed to catalyze sequential aldol reactions with non-natural substrates, the catalytic efficiency is quite low, which restricts its practical applicability. Consequently, scaling up the reaction was required to obtain sufficient amounts of material for successful purification [28].

Following scale-up, the lactol product **6i** was isolated from an 8 mL reaction mixture through an extensive work-up and chromatographic purification. Due to the high polarity of the nucleoside scaffold and the lability of the hemiacetal function, the crude reaction mixture was first subjected to multiple extractions with ethyl acetate. The combined organic phases were dried, filtered, and concentrated under reduced pressure. The resulting residue was purified by column chromatography on silica gel (230 mesh), using approximately 40% *w*/*w* of crude material relative to the stationary phase. Elution was performed using dichloromethane/methanol as the mobile phase, gradually increasing the polarity until a final ratio of 90:10 was reached. Column progress was monitored by TLC, using dichloromethane/methanol (9:1) as the eluent, where the desired lactol exhibited an R*f* value of 0.20. The product was obtained as a colorless, viscous liquid in 28% yield.

$^{1}$H and $^{13}$C NMR spectroscopic analyses confirmed the successful isolation of the lactol product and revealed the presence of a mixture of anomeric forms resulting from cyclization of the thymine-substituted lactol (Figures S8–S11). The observed α/β anomeric ratio is consistent with that previously reported for related substituted lactols bearing different R groups [60]. As shown in Figure 2, the $^{1}$H NMR spectrum of an anomerically enriched mixture clearly displays the signal corresponding to the major anomer, appearing as a doublet with a coupling constant of 9.1 Hz, which is characteristic of the α-anomer. In the expanded region of this part of the spectrum, a significantly weaker signal attributable to the β-anomer can also be observed. Minor impurities attributable to residual TDHP were also detected in the crude material but were effectively removed during chromatographic purification.

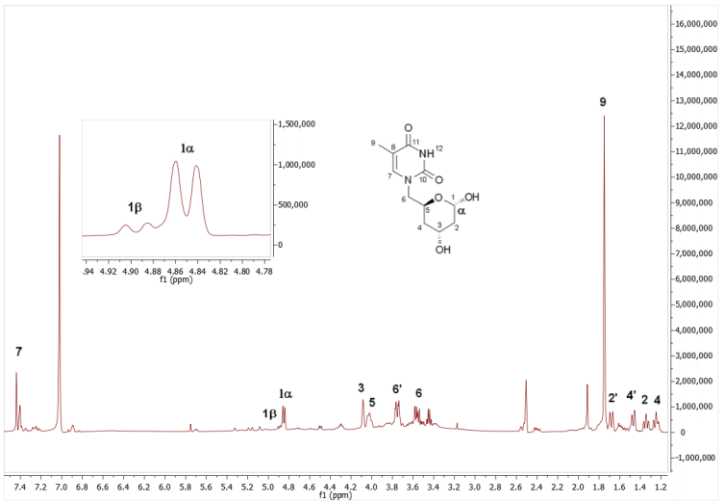


**Figure 2.** Partial view of the $^{1}$H NMR spectrum of **6i** obtained by *Pa*DERA C49M biocatalyzed aldol addition of **5i** and acetaldehyde as substrates. The inset shows C1 hydrogen signals of the anomers.

The scale up and purification of 6ii and 6iii still remain a challenge, mainly due to the low conversions observed for the corresponding nucleobase-derived aldehydes, which reached 5% for the adenine derivative (6ii) and below 2% for the cytosine analogue (6iii), as determined by HPLC analysis.

## 4. Conclusions

In this work, a novel chemoenzymatic strategy was developed for the synthesis of nucleobase-substituted lactol products as potential precursors of new statin analogues. The C49M variant of 2-deoxyribose-5-phosphate aldolase from *Pectobacterium atrosepticum* (*Pa*DERA C49M) was demonstrated to catalyze aldol reactions involving aldehyde-functionalized nucleobases as non-natural electrophilic substrates, thereby expanding

the substrate scope of DERA beyond conventional electrophiles and providing access to previously unexplored statin side-chain architectures.

Notably, the methodology presented here introduces a distinct approach to statin synthesis, as the lateral chain is constructed directly from substrates already bearing the heterocyclic moiety. By incorporating the nucleobase at an early stage, this strategy avoids post-aldol coupling steps commonly required in traditional synthetic routes, which often result in longer, less efficient, and lower-yielding synthetic sequences.

While significant progress has been achieved in improving DERA stability, particularly through the use of enzymes from thermophilic organisms or via random mutagenesis, several challenges must still be addressed before DERA can be considered a robust and broadly applicable industrial biocatalyst. These include limitations in catalytic efficiency with non-natural substrates, product stability, and downstream processing.

Looking forward, constant efforts focus on enzyme optimization and reaction engineering to improve productivity and selectivity. In parallel, the lactol oxidation to lactone and the biological evaluation of the newly synthesized nucleobase-containing statin analogues are currently in progress, with the aim of assessing their pharmacological potential and identifying promising candidates for further development.

**Supplementary Materials:** The following supporting information can be downloaded at https://www.mdpi.com/article/10.3390/biom16020321/s1, Figure S1: DNA sequence of *Pectobacterium atrosepticum* DERA. Figure S2: Amino acid sequences of *Pa*DERA and *Pa*DERA C49M. Figure S3: SDS–PAGE analysis of batch purification fractions. Lane 1: non-bound fraction (flow-through) after batch binding to Ni–Sepharose resin; lanes 2–3: wash fractions (5 and 20 mM imidazole); lanes 4–6: elution fractions (100, 250, and 500 mM imidazole); lane 7: molecular weight marker. Cell-free extract was not loaded; only purification fractions are shown. Figure S4: $^{1}$H NMR analysis of **2a**: 2,4,6-trideoxy-D-erythro-hexapyranose obtained with DERA as biocatalyst. **Figure S5**: $^{13}$C NMR analysis of **2a**: 2,4,6-trideoxy-D-erythro-hexapyranose obtained with DERA as biocatalyst. Figure S6: $^{1}$H NMR analysis of **2b**: 6-chloro-2,4,6-trideoxy-D-erythro-hexapyranose obtained with DERA as biocatalyst. Figure S7: $^{13}$C NMR analysis of **2b**: 6-chloro-2,4,6-trideoxy-D-erythro-hexapyranose obtained with DERA as biocatalyst. Figure S8: $^{1}$H NMR analysis of **6i**: 6-thyminyl-2,4,6-trideoxy-D-erythro-hexopyranose obtained with DERA as biocatalyst. **Figure S9**: $^{13}$C NMR analysis of **6i**: 6-thyminyl-2,4,6-trideoxy-D-erythro-hexopyranose obtained with DERA as biocatalyst. **Figure S10**: HSQC NMR analysis of **6i**: 6-thyminyl-2,4,6-trideoxy-D-erythro-hexopyranose obtained with DERA as biocatalyst. Figure S11: gCOSY NMR analysis of **6i**: 6-thyminyl-2,4,6-trideoxy-D-erythro-hexopyranose obtained with DERA as biocatalyst. Figure S12: $^{1}$H NMR analysis of **4i**: *N*-1-(2,2-dimethoxyethyl) thymine obtained by chemical synthesis. Figure S13: $^{1}$H NMR analysis of **4ii**: *N*-1-(2,2-dimethoxyethyl) cytosine obtained by chemical synthesis. Figure S14: $^{13}$C NMR analysis of **4ii**: *N*-1-(2,2-dimethoxyethyl) cytosine obtained by chemical synthesis. **Figure S15**: $^{1}$H NMR analysis of **4iii**: *N*-9-(2,2-dimethoxyethyl) adenine obtained by chemical synthesis. Figure S16: $^{13}$C NMR analysis of **4iii:** *N*-9-(2,2-dimethoxyethyl) adenine obtained by chemical synthesis. **Figure S17**: GC analysis of **2a**: 2,4,6-trideoxy-D-erythro-hexapyranose (TDHP). Rt: 13.9 min. Figure S18: GC analysis of **2c**: 6-methyl-2,4,6-trideoxy-D-erythro-hexapyranose. Rt: 15.3 min. Figure S19: GC analysis of **2d**: 6-phenyl-2,4,6-trideoxy-D-erythro-hexapyranose. Rt: 18.7 min. Figure S20: LC-ESI-MS analysis for **6i**: 6-thyminyl-2,4,6-trideoxy-D-erythro-hexapyranose. (A) Total ion chromatogram in the positive mode for compound **6i** at Rt 7.49 min. (B) Mass spectra found as $[M + H^+]$ corresponding to the product $[C_{11}H_{17}N_2O_5]^+$: 257.1124). Figure S21: LC-ESI-MS analysis for **6ii**: 6-cytosyl-2,4,6-trideoxy-D-erythro-hexapyranose. A) Total ion chromatogram in the positive mode for compound **6ii** at Rt 3.19 min. B) Mass spectra found as $[M - H^+]$ corresponding to the product $[C_{10}H_{16}N_3O_4]^+$: 242.1127). Figure S22: LC-ESI-MS analysis for **6iii**: 6-adenyl-2,4,6-trideoxy-D-erythro-hexapyranose. A) Total ion chromatogram in the positive mode for compound 6iii at Rt 8.27 min. B) Mass spectra found as $[M + H^+]$ corresponding to the product $[C_{11}H_{16}N_5O_3]^+$: 266.1240). Table S1: The qualitative analysis of whole-cell biotransformations (**2a-d**) was performed by TLC using acetonitrile:ethylether

1:1 ($v/v$) as a solvent and the spots were visualized by heating after spraying with 5 % $v/v$ $H_2SO_4$ in ethanol. Table S2: The qualitative analysis of free-enzyme biotransformations was performed by TLC using dichloromethane:methanol 9:1 ($v/v$) as solvent and the spots were visualized by UV light. Table S3: The qualitative analysis of substrate synthesis was performed by TLC using dichloromethane:methanol 9:1 ($v/v$) as solvent and the spots were visualized by UV light.

**Author Contributions:** Performed the experiments, R.F.V., E.A., L.G., L.C. and L.L.; writing—review and editing, R.F.V., E.A., P.-L.H., U.H., L.G., L.L., A.L.V. and E.L.; funding acquisition and supervision, U.H., A.I. and E.L. All authors have read and agreed to the published version of the manuscript.

**Funding:** This work was supported by Universidad Nacional de Quilmes (PP I+D 2287/22), Agencia Nacional de Promoción Científica y Tecnológica, ANPCYT, (PICT 2019 1361 and PICT 2021 0984), National Council of Science and Technology, CONICET (11220200101081CO), Argentina, and ER-ACoBiotech (grant 053.80.737; BioDiMet); L.L., A.I. and E.S.L. are research members of CONICET; L.A.M.G. and R.N.F.V are CONICET fellows.

**Institutional Review Board Statement:** Not applicable.

**Informed Consent Statement:** Not applicable.

**Data Availability Statement:** The original contributions presented in this study are included in the article/Supplementary Materials. Further inquiries can be directed to the corresponding author.

**Conflicts of Interest:** The authors declare no conflicts of interest.

## References

1. Laranjo, L.; Lanas, F.; Sun, M.C.; Chen, D.A.; Hynes, L.; Imran, T.F.; Kazi, D.S.; Kengne, A.P.; Komiyama, M.; Kuwabara, M.; et al. World Heart Federation Roadmap for Secondary Prevention of Cardiovascular Disease: 2023 Update. *Glob. Heart* **2024**, *19*, 8. [CrossRef] [PubMed]
2. Di Cesare, M.; McGhie, D.V.; Perel, P.; Mwangi, J.; Taylor, S.; Pervan, B.; Kabudula, C.; Narula, J.; Bixby, H.; Pineiro, D.; et al. The Heart of the World. *Glob. Heart* **2024**, *19*, 11. [CrossRef] [PubMed]
3. Münzel, T.; Sørensen, M.; Lelieveld, J.; Landrigan, P.J.; Kuntic, M.; Nieuwenhuijsen, M.; Miller, M.R.; Schneider, A.; Daiber, A. A Comprehensive Review/Expert Statement on Environmental Risk Factors of Cardiovascular Disease. *Cardiovasc. Res.* **2025**, *121*, 1653–1678. [CrossRef]
4. Virani, S.S.; Ramsey, D.J.; Westerman, D.; Kuebeler, M.K.; Chen, L.; Akeroyd, J.M.; Gobbel, G.T.; Ballantyne, C.M.; Petersen, L.A.; Turchin, A.; et al. Cluster Randomized Trial of a Personalized Clinical Decision Support Intervention to Improve Statin Prescribing in Patients with Atherosclerotic Cardiovascular Disease. *Circulation* **2023**, *147*, 1411–1413. [CrossRef] [PubMed]
5. Tang, X.L.; Yu, J.W.; Geng, Y.H.; Wang, J.R.; Zheng, R.C.; Zheng, Y.G. From Discovery to Mass Production: A Perspective on Bio-Manufacturing Exemplified by the Development of Statins. *Engineering* **2023**, *24*, 138–150. [CrossRef]
6. Zeng, W.; Deng, H.; Luo, Y.; Zhong, S.; Huang, M.; Tomlinson, B. Advances in Statin Adverse Reactions and the Potential Mechanisms: A Systematic Review. *J. Adv. Res.* **2025**, *76*, 781–797. [CrossRef]
7. Ward, N.C.; Watts, G.F.; Eckel, R.H. Statin Toxicity: Mechanistic Insights and Clinical Implications. *Circ. Res.* **2019**, *124*, 328–350. [CrossRef]
8. Kim, T.; Stogios, P.J.; Khusnutdinova, A.N.; Nemr, K.; Skarina, T.; Flick, R.; Joo, J.C.; Mahadevan, R.; Savchenko, A.; Yakunin, A.F. Rational Engineering of 2-Deoxyribose-5-Phosphate Aldolases for the Biosynthesis of (R)-1,3-Butanediol. *J. Biol. Chem.* **2020**, *295*, 597–609. [CrossRef]
9. Roldán, R.; Sanchez-Moreno, I.; Scheidt, T.; Hélaine, V.; Lemaire, M.; Parella, T.; Clapés, P.; Fessner, W.D.; Guérard-Hélaine, C. Breaking the Dogma of Aldolase Specificity: Simple Aliphatic Ketones and Aldehydes Are Nucleophiles for Fructose-6-Phosphate Aldolase. *Chem.-A Eur. J.* **2017**, *23*, 5005–5009. [CrossRef]
10. Chambre, D.; Guérard-Hélaine, C.; Darii, E.; Mariage, A.; Petit, J.L.; Salanoubat, M.; De Berardinis, V.; Lemaire, M.; Hélaine, V. 2-Deoxyribose-5-Phosphate Aldolase, a Remarkably Tolerant Aldolase towards Nucleophile Substrates. *Chem. Commun.* **2019**, *55*, 7498–7501. [CrossRef]
11. Haridas, M.; Abdelraheem, E.M.M.; Hanefeld, U. 2-Deoxy-d-Ribose-5-Phosphate Aldolase (DERA): Applications and Modifications. *Appl. Microbiol. Biotechnol.* **2018**, *102*, 9959–9971. [CrossRef] [PubMed]
12. Laurent, V.; Hélaine, V.; Vergne-Vaxelaire, C.; Nauton, L.; Traikia, M.; Petit, J.L.; Salanoubat, M.; De Berardinis, V.; Lemaire, M.; Guérard-Hélaine, C. Achiral Hydroxypyruvaldehyde Phosphate as a Platform for Multi-Aldolases Cascade Synthesis of Diuloses

and for a Quadruple Acetaldehyde Addition Catalyzed by 2-Deoxyribose-5-Phosphate Aldolases. *ACS Catal.* **2019**, *9*, 9508–9512. [CrossRef]
13. Gijsen, H.J.M.; Wong, C.H. Sequential One-Pot Aldol Reactions Catalyzed by 2-Deoxyribose-5-Phosphate Aldolase and Fructose-1,6-Diphosphate Aldolase. *J. Am. Chem. Soc.* **1995**, *117*, 2947–2948. [CrossRef]
14. Patel, R.N. Biocatalysis for Synthesis of Pharmaceuticals. *Bioorg. Med. Chem.* **2018**, *26*, 1252–1274. [CrossRef]
15. Wong, C.H.; Garcia-Junceda, E.; Chen, L.; Blanco, O.; Gijsen, H.J.; Steensma, D.H. Recombinant 2-deoxyribose-5-phosphate aldolase in organic synthesis: Use of sequential two-substrate and three-substrate aldol reactions. *J. Am. Chem. Soc.* **1995**, *12*, 3333–3339. [CrossRef]
16. Dick, M.; Hartmann, R.; Weiergräber, O.H.; Bisterfeld, C.; Classen, T.; Schwarten, M.; Neudecker, P.; Willbold, D.; Pietruszka, J. Mechanism-Based Inhibition of an Aldolase at High Concentrations of Its Natural Substrate Acetaldehyde: Structural Insights and Protective Strategies. *Chem. Sci.* **2016**, *7*, 4492–4502. [CrossRef]
17. Fei, H.; Zheng, C.C.; Liu, X.Y.; Li, Q. An Industrially Applied Biocatalyst: 2-Deoxy-D-Ribose-5- Phosphate Aldolase. *Process Biochem.* **2017**, *63*, 55–59. [CrossRef]
18. Voutilainen, S.; Heinonen, M.; Andberg, M.; Jokinen, E.; Maaheimo, H.; Pääkkönen, J.; Hakulinen, N.; Rouvinen, J.; Lähdesmäki, H.; Kaski, S.; et al. Substrate Specificity of 2-Deoxy-D-Ribose 5-Phosphate Aldolase (DERA) Assessed by Different Protein Engineering and Machine Learning Methods. *Appl. Microbiol. Biotechnol.* **2020**, *104*, 10515–10529. [CrossRef]
19. He, F.F.; Xin, Y.Y.; Ma, Y.X.; Yang, S.; Fei, H. Rational Design to Enhance the Catalytic Activity of 2-Deoxy-D-Ribose-5-Phosphate Aldolase from *Pseudomonas syringae pv. syringae* B728a. *Protein Expr. Purif.* **2021**, *183*, 105863. [CrossRef]
20. Yin, X.; Wang, Q.; Zhao, S.J.; Du, P.F.; Xie, K.L.; Jin, P.; Xie, T. Cloning and Characterization of a Thermostable 2-Deoxy-D-Ribose-5-Phosphate Aldolase from *Aciduliprofundum boonei*. *Afr. J. Biotechnol.* **2011**, *10*, 16260–16266. [CrossRef]
21. Bramski, J.; Dick, M.; Pietruszka, J.; Classen, T. Probing the Acetaldehyde-Sensitivity of 2-Deoxy-Ribose-5-Phosphate Aldolase (DERA) Leads to Resistant Variants. *J. Biotechnol.* **2017**, *258*, 56–58. [CrossRef] [PubMed]
22. Jiao, X.C.; Pan, J.; Kong, X.D.; Xu, J.H. Protein Engineering of Aldolase LbDERA for Enhanced Activity toward Real Substrates with a High-Throughput Screening Method Coupled with an Aldehyde Dehydrogenase. *Biochem. Biophys. Res. Commun.* **2017**, *482*, 159–163. [CrossRef] [PubMed]
23. Kullartz, I.; Pietruszka, J. Cloning and Characterisation of a New 2-Deoxy-d-Ribose-5-Phosphate Aldolase from *Rhodococcus erythropolis*. *J. Biotechnol.* **2012**, *161*, 174–180. [CrossRef] [PubMed]
24. Sakuraba, H.; Yoneda, K.; Yoshihara, K.; Satoh, K.; Kawakami, R.; Uto, Y.; Tsuge, H.; Takahashi, K.; Hori, H.; Ohshima, T. Sequential Aldol Condensation Catalyzed by Hyperthermophilic 2-Deoxy-D-Ribose-5-Phosphate Aldolase. *Appl. Environ. Microbiol.* **2007**, *73*, 7427–7434. [CrossRef]
25. Sakuraba, H.; Tsuge, H.; Shimoya, I.; Kawakami, R.; Goda, S.; Kawarabayasi, Y.; Katunuma, N.; Ago, H.; Miyano, M.; Ohshima, T. The First Crystal Structure of Archaeal Aldolase. Unique Tetrameric Structure of 2-Deoxy-D-Ribose-5-Phosphate Aldolase from the Hyperthermophilic Archaea *Aeropyrum pernix*. *J. Biol. Chem.* **2003**, *278*, 10799–10806. [CrossRef]
26. Han, L.; Chen, X.; Feng, J.; Wu, Q.; Zhu, D. Cloning, Purification and Characterization of Promising 2-Deoxy-D-Ribose 5-Phosphate Aldolase from *Staphylococcus aureus* N315. *Chin. J. Bioprocess Eng* **2013**, *11*, 47–53.
27. Valino, A.L.; Palazzolo, M.A.; Iribarren, A.M.; Lewkowicz, E. Selection of a New Whole Cell Biocatalyst for the Synthesis of 2-Deoxyribose 5-Phosphate. *Appl. Biochem. Biotechnol.* **2012**, *166*, 300–308. [CrossRef]
28. Haridas, M.; Bisterfeld, C.; Chen, L.M.; Marsden, S.R.; Tonin, F.; Médici, R.; Iribarren, A.; Lewkowicz, E.; Hagedoorn, P.-L.; Hanefeld, U.; et al. Discovery and Engineering of an Aldehyde Tolerant 2-Deoxy-D-Ribose 5-Phosphate Aldolase (DERA) from *Pectobacterium atrosepticum*. *Catalysts* **2020**, *10*, 883. [CrossRef]
29. Rouvinen, J.; Andberg, M.; Pääkkönen, J.; Hakulinen, N.; Koivula, A. Current State of and Need for Enzyme Engineering of 2-Deoxy-D-Ribose 5-Phosphate Aldolases and Its Impact. *Appl. Microbiol. Biotechnol.* **2021**, *105*, 6215–6228. [CrossRef]
30. Greenberg, W.A.; Varvak, A.; Hanson, S.R.; Wong, K.; Huang, H.; Chen, P.; Burk, M.J. Development of an Efficient, Scalable, Aldolase-Catalyzed Process for Enantioselective Synthesis of Statin Intermediates. *Proc. Natl. Acad. Sci. USA* **2004**, *101*, 5788–5793. [CrossRef]
31. Jennewein, S.; Schürmann, M.; Wolberg, M.; Hilker, I.; Luiten, R.; Wubbolts, M.; Mink, D. Directed Evolution of an Industrial Biocatalyst 2-Deoxy-d-Ribose 5-Phosphate Aldolase. *Biotechnol. J.* **2006**, *1*, 537–548. [CrossRef]
32. Jiao, X.C.; Pan, J.; Xu, G.C.; Kong, X.D.; Chen, Q.; Zhang, Z.J.; Xu, J.H. Efficient Synthesis of a Statin Precursor in High Space-Time Yield by a New Aldehyde-Tolerant Aldolase Identified from *Lactobacillus brevis*. *Catal. Sci. Technol.* **2015**, *5*, 4048–4054. [CrossRef]
33. Xuan, K.; Yang, G.; Wu, Z.; Xu, Y.; Zhang, R. Efficient Synthesis of (3R,5S)-6-Chloro-2,4,6-Trideoxyhexapyranose by Using New 2-Deoxy-D-Ribose-5-Phosphate Aldolase from *Streptococcus Suis* with Moderate Activity and Aldehyde Tolerance. *Process Biochem.* **2020**, *92*, 113–119. [CrossRef]
34. Švarc, A.; Fekete, M.; Hernandez, K.; Clapés, P.; Findrik Blažević, Z.; Szekrenyi, A.; Skendrović, D.; Vasić-Rački, Đ.; Charnock, S.J.; Presečki, A.V. An Innovative Route for the Production of Atorvastatin Side-Chain Precursor by DERA-Catalysed Double Aldol Addition. *Chem. Eng. Sci.* **2021**, *231*, 116312. [CrossRef]

35. Ošlaj, M.; Cluzeau, J.; Orkić, D.; Kopitar, G.; Mrak, P.; Časar, Z. A Highly Productive, Whole-Cell DERA Chemoenzymatic Process for Production of Key Lactonized Side-Chain Intermediates in Statin Synthesis. *PLoS ONE* **2013**, *8*, e62250. [CrossRef]
36. Liu, J.; Hsu, C.C.; Wong, C.H. Sequential Aldol Condensation Catalyzed by DERA Mutant Ser238Asp and a Formal Total Synthesis of Atorvastatin. *Tetrahedron Lett.* **2004**, *45*, 2439–2441. [CrossRef]
37. Bauer, D.W.; O'Nell, P.M.; Watson, T.J.; Hu, S. Title of Patent Process for preparing chiral compounds. U.S. Patent 8,642,783 B2, 4 February 2014.
38. Ručigaj, A.; Krajnc, M. Optimization of a Crude Deoxyribose-5-Phosphate Aldolase Lyzate-Catalyzed Process in Synthesis of Statin Intermediates. *Org. Process Res. Dev.* **2013**, *17*, 854–862. [CrossRef]
39. García-Bofill, M.; Sutton, P.W.; Guillén, M.; Álvaro, G. Enzymatic Synthesis of a Statin Precursor by Immobilised Alcohol Dehydrogenase with NADPH Oxidase as Cofactor Regeneration System. *Appl. Catal. A Gen.* **2021**, *609*, 117909. [CrossRef]
40. Istvan, E.S.; Deisenhofer, J. Structural Mechanism for Statin Inhibition of HMG-CoA Reductase. *Science* **2001**, *292*, 1160–1164. [CrossRef]
41. Sadowska, A.; Osiński, P.; Roztocka, A.; Kaczmarz-Chojnacka, K.; Zapora, E.; Sawicka, D.; Car, H. Statins—From Fungi to Pharmacy. *Int. J. Mol. Sci.* **2023**, *25*, 466–491. [CrossRef]
42. Li, X.Z.; Jiang, S.Y.; Li, G.Q.; Jiang, Q.R.; Li, J.W.; Li, C.C.; Han, Y.Q.; Song, B.L.; Ma, X.R.; Qi, W.; et al. Synthesis of Heterocyclic Ring-Fused Analogs of HMG499 as Novel Degraders of HMG-CoA Reductase That Lower Cholesterol. *Eur. J. Med. Chem.* **2022**, *236*, 114323. [CrossRef]
43. Yamada, T.; Komoto, J.; Lou, K.; Ueki, A.; Hua, D.H.; Sugiyama, K.; Takata, Y.; Ogawa, H.; Takusagawa, F. Structure and Function of Eritadenine and Its 3-Deaza Analogues: Potent Inhibitors of S-Adenosylhomocysteine Hydrolase and Hypocholesterolemic Agents. *Biochem. Pharmacol.* **2007**, *73*, 981–989. [CrossRef] [PubMed]
44. Ishara, J.; Buzera, A.; Mushagalusa, G.N.; Hammam, A.R.; Munga, J.; Karanja, P.; Kinyuru, J. Nutraceutical Potential of Mushroom Bioactive Metabolites and Their Food Functionality. *J. Food Biochem.* **2022**, *46*, e14025. [CrossRef] [PubMed]
45. Fernández Varela, R.; Valino, A.L.; Abdelraheem, E.; Médici, R.; Sayé, M.; Pereira, C.A.; Hagedoorn, P.; Hanefeld, U.; Iribarren, A.; Lewkowicz, E. Synthetic Activity of Recombinant Whole Cell Biocatalysts Containing 2-Deoxy-D-ribose-5-phosphate Aldolase from *Pectobacterium atrosepticum*. *ChemBioChem* **2022**, *23*, e202200147. [CrossRef] [PubMed]
46. Švarc, A.; Findrik Blažević, Z.; Vasić-Rački, Đ.; Szekrenyi, A.; Fessner, W.D.; Charnock, S.J.; Vrsalović Presečki, A. 2-Deoxyribose-5-Phosphate Aldolase from Thermotoga Maritima in the Synthesis of a Statin Side-Chain Precursor: Characterization, Modeling and Optimization. *J. Chem. Technol. Biotechnol.* **2019**, *94*, 1832–1842. [CrossRef]
47. Bradford, M.M. A Rapid and Sensitive Method for the Quantitation of Microgram Quantities of Protein Utilizing the Principle of Protein-Dye Binding. *Anal. Biochem.* **1976**, *72*, 248–254. [CrossRef]
48. Palazzolo, M.A.; Nigro, M.J.; Iribarren, A.M.; Lewkowicz, E.S. A Chemoenzymatic Route to Prepare Acyclic Nucleoside Analogues. *Eur. J. Org. Chem.* **2016**, *2016*, 921–924. [CrossRef]
49. Nigro, M.J.; Brardinelli, J.I.; Lewkowicz, E.S.; Iribarren, A.M.; Laurella, S.L. Aldehyde-Hydrate Equilibrium in Nucleobase 2-Oxoethyl Derivatives: An NMR, ESI-MS and Theoretical Study. *J. Mol. Struct.* **2017**, *1144*, 49–57. [CrossRef]
50. Butler, D.E.; Le, T.V.; Millar, A.; Nanninga, T.N. Title of Patent: Process for the synthesis of (5R)-1,1-dimethylethyl-6-cyano-5-hydroxy-3-oxo-hexanoate. U.S. Patent 5155251, 13 October 1992.
51. Wolberg, M.; Filho, M.V.; Bode, S.; Geilenkirchen, P.; Feldmann, R.; Liese, A.; Hummel, W.; Müller, M. Chemoenzymatic Synthesis of the Chiral Side-Chain of Statins: Application of an Alcohol Dehydrogenase Catalysed Ketone Reduction on a Large Scale. *Bioprocess Biosyst. Eng.* **2008**, *31*, 183–191. [CrossRef]
52. Hoyos, P.; Pace, V.; Alcántara, A.R. Biocatalyzed Synthesis of Statins: A Sustainable Strategy for the Preparation of Valuable Drugs. *Catalysts* **2019**, *9*, 260. [CrossRef]
53. Rizzo, A.; Aranda, C.; Galman, J.; Alcasabas, A.; Pandya, A.; Bornadel, A.; Costa, B.; Hailes, H.C.; Ward, J.M.; Jeffries, J.W.E.; et al. Broadening the Substrate Scope of Aldolases Through Metagenomic Enzyme Discovery. *ChemBioChem* **2024**, *25*, e202400278. [CrossRef] [PubMed]
54. Hélaine, V.; Gastaldi, C.; Lemaire, M.; Clapés, P.; Guérard-Hélaine, C. Recent Advances in the Substrate Selectivity of Aldolases. *ACS Catal.* **2022**, *12*, 733–761. [CrossRef]
55. Schulte, M.; Petrović, D.; Neudecker, P.; Hartmann, R.; Pietruszka, J.; Willbold, S.; Willbold, D.; Panwalkar, V. Conformational Sampling of the Intrinsically Disordered C-Terminal Tail of DERA Is Important for Enzyme Catalysis. *ACS Catal.* **2018**, *8*, 3971–3984. [CrossRef] [PubMed]
56. Abdelraheem, E.; Kuijpers, R.; Hagedoorn, P.L.; Hollmann, F.; Hanefeld, U. Enzymatic Cascade of DERA and ADH for Lactone Synthesis. *Catal. Sci. Technol.* **2024**, *14*, 2739–2751. [CrossRef]
57. Müller, M. Chemoenzymatic Synthesis of Building Blocks for Statin Side Chains. *Angew. Chem.-Int. Ed.* **2005**, *44*, 362–365. [CrossRef]
58. Nigro, M.J.; Palazzolo, M.A.; Colasurdo, D.; Iribarren, A.M.; Lewkowicz, E.S. N-Acetylneuraminic Acid Aldolase-Catalyzed Synthesis of Acyclic Nucleoside Analogues Carrying a 4-Hydroxy-2-Oxoacid Moiety. *Catal. Commun.* **2019**, *121*, 73–77. [CrossRef]

59. Nigro, M.; Sánchez-Moreno, I.; Benito-Arenas, R.; Valino, A.L.; Iribarren, A.M.; Veiga, N.; García-Junceda, E.; Lewkowicz, E.S. Synthesis of Chiral Acyclic Pyrimidine Nucleoside Analogues from DHAP-Dependent Aldolases. *Biomolecules* **2024**, *14*, 750. [CrossRef]
60. Rosen, T.; Taschner, M.J. Synthetic and Biological Studies of Compactin and Related Compounds. 2. Synthesis of the Lactone Moiety of Compactin. *J. Org. Chem.* **1984**, *21*, 3994–4003. [CrossRef]